Proceedings of ASME Turbo Expo 2011
GT2011
June 6-10, 2011, Vancouver, British Columbia, Canada

GT2011-45107

DESIGN AND VALIDATION OF A NEW TEST RIG FOR BRUSH SEAL TESTING UNDER ENGINE RELEVANT CONDITIONS

D. Pfefferle, K. Dullenkopf, H.-J. Bauer
Institut für Thermische Strömungsmaschinen
Karlsruher Institut für Technologie (KIT)
76131 Karlsruhe, Germany

ABSTRACT

Brush seals play an increasing role in turbomachinery due to their improved behavior towards leakage and their capability to compensate for gap variations caused by thermal expansion and rotor excursions. The flexible bristles of brush seals are able to endure short-term reductions in gap width without severe damage. Consequently the necessary gap between the rotor and brush seal can virtually be reduced to zero, leading to a considerable reduction in air leakage of up to 80 percent. However the reduced gap height increases the probability of rubbing between the bristle package and the rotor surface. The friction forces generated can cause an unwanted heat load on the rotor, bristles and leakage air. In addition, the surfaces involved are exposed to abrasion effects. Especially in the thin and lightweight rotor structures of aircraft engines, the additional heat impact can lead to a problematic level of material stress. To study these effects and to give reliable quantitative design rules, a versatile test rig for brush seals was designed and built. The simulation of seal behavior under relevant engine conditions is the main emphasis of this rig, including high pressure drop, leakage flow and high surface speed. The key feature is the possibility to vary the axis symmetric radial gap width during the test rig operation by up to a 0.5 mm overlap. The so caused rubbing induces a transient rotor temperature rise which is measured via a set of 12 thermocouples embedded in the rotor. These temperature readings can be used to calculate the brush seal heat impact on the rotor structure. Preliminary results with moderate differential pressure and rotor speed proved the functionality of the test rig and confirmed the global approach of the project.

INTRODUCTION

Undesired leakage flows in turbo machines greatly contribute to the overall efficiency losses. Hence improving the seal performance enables higher engine performance in terms of decreased specific fuel consumption and higher thrust [1]. Therefore, the efficient use of secondary air whilst reducing leakage flow is a crucial point in today's, and future, engine generation. Currently used seals, such as labyrinth seals, have reached their limits due to the inherent gap between the sealing fins and the stator surface. This gap cannot be reduced further for reasons of thermal expansion, rotor eccentricity and - in aero engines - maneuver forces.

NOMENCLATURE

Δp	Differential pressure
u	Rotational speed
Δs	Rotor – seal overlap
Δt_1	Time span from start to steady-state
Δt_2	Time span of brush seal rubbing
Δt_3	Time span of rotor cool-down
B	Bristle package width
d	Single bristle diameter
TC 1 … TC 6	Thermocouple No. 1 – No. 6
Φ	Bristle inclination angle

Benefits of brush seals

Amongst other alternatives to labyrinth seals, brush seals have already proven their great potential to dramatically reduce leakage [2][3]. Their development and design has been thoroughly discussed in the literature, e.g. [4][5][6][7][8]. As can be seen in Fig. 1, the seal consists of a compliant bristle structure, mounted between a backing plate and a front plate.
Depending on the supplier, the bristles are connected to the casing by either welding, bracing or clamping. The flexible bristle structure can cope with short-term rotor interference without being irreversibly damaged. Hence it is possible to

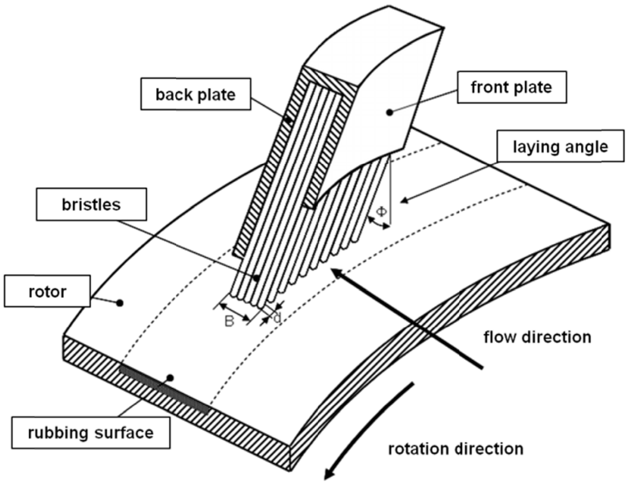

Fig. 1: Typical brush seal arrangement

reduce the gap between the bristle package and the rotor surface to virtually zero, resulting in a reduction of leakage of up to 80% [9]. This is mainly due to the dense arrangement of the bristles, which represent a high flow resistance. Even in the case of partial or total bristle loss, the backing plate works as emergency (labyrinth) seal, which makes the brush seal a reliable concept. In addition to the reduced leakage, a brush seal features further advantages; it is lightweight, axially compact and enhances rotor dynamic behavior.

Brush seal heat impact on thin rotor structures

In aero engines, inner air seals are often placed on thin walled structures, which in some cases serve as well as a drive arm connection between turbine discs (see Fig. 2). As conventional labyrinth seals do not create a major frictional heat impact when operated properly, this design is used by many manufacturers across complete engine families. Compared to labyrinth seals, brush seals show a dramatic reduction in air leakage. This led to a couple of (military) applications in engines like the RB199 and EJ200. The secondary air consumption has a large effect on the engine efficiency [1]. Consequently, it would be beneficial if brush seals could be used without limitations as replacement for existing seals. However, in contrast to labyrinth seals, the very small gap between the bristles and the rotor surface leads to an unavoidable rotor-seal contact. This contact occurs especially after mounting a new brush seal, during engine transients or eccentric operation, and is further driven by the blow-down effect [11][12]. The problem of rotor-brush interaction has been addressed by a variety of publications [13][14][15]. As long as the frictional heat is dissipated by the rotor structure and the air leakage, a certain degree of interference can be tolerated. Using massive shafts like in stationary turbines, this is normally no problem. However, for thin walled sealing positions, like in aircraft engines where mostly nickel based materials are used, heat impact through brush seal rubbing can be a severe problem

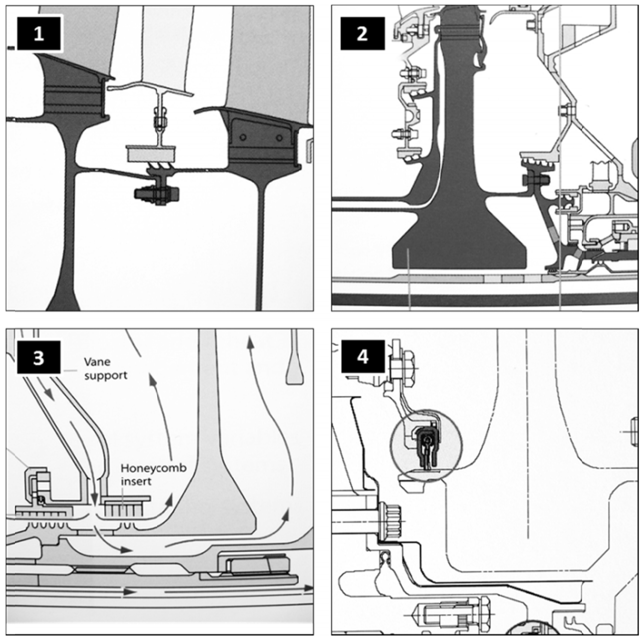

Fig. 2: Seal arrangements in aero engines.
1-3: RR engines [10], 4: EJ200 brush seal [9]

[15]. The effects of frictional heat impact on the material stress if such thin walled structures shall be shown in the following paragraph.

A simple finite elements model was set up, and used with typical data from a turbojet engine. The model assumes a rotor disc with a thin sealing surface of Ø200 mm, which is operated with a brush seal. The brush seal is assumed to be operated with strong interference causing heat impact into the structure of 8 kW. The rotational speed is 18.000 rpm and the disc has an initial temperature of between 750 K and 800 K before the brush seal heat impact starts. The heat impact is maintained for 100 s. The heat transfer coefficient at all surfaces was set to 500 W/(mK) with an ambient temperature of 750 K. The model includes precise, temperature-dependent material data from Inconel 718. The results of the analysis are shown in Fig. 3. The disc is exposed to a heat load leading to high temperature gradients, a hot spot of over 1800 K at the rubbing surface, and very high local material stress of up to 1000 MPa. Already exposed to high mechanical and thermal loads, the additional frictional heat impact cannot be dissipated quickly enough. The reason for the high temperature gradient is mainly the low heat transfer coefficient of Inconel718 (and other similar alloys).

Due to some model simplifications, this simulation is not intended to give highly accurate results. It does not consider variable heat transfer coefficients, and it assumes a high heat impact on the rotor disc. Despite the simplifications, the model shows a worst case scenario of a brush seal operated with heavy rotor interference. Considering the effects of strong rubbing, the

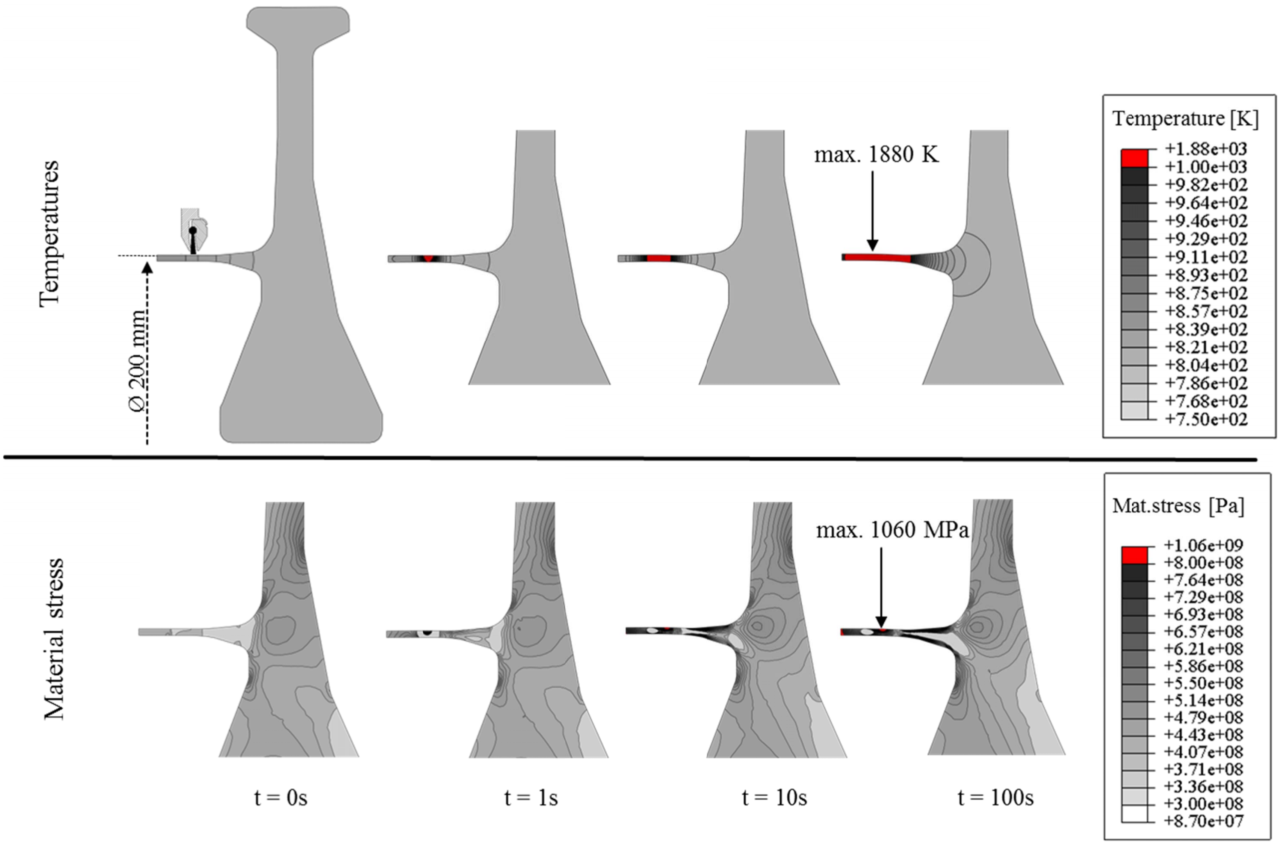

Fig. 3: Effect of brush seal interference with a rotating disc

simulation justifies the thorough analysis which will be performed at the Institut für Thermische Strömungsmaschinen (ITS).

APPROACH

Concerning the heat impact of brush seals, the available literature covers detailed analysis of singular aspects like brush seal bristle mechanics (e.g. bristle-rotor contact forces [16][17][18]). Other authors have addressed temperature distribution models based on CFD calculations with a porous media approach [15]. Furthermore, achievements in experimental research have been made, providing data about brush seal heat impact on the rotor disc for different brush seal types and pressure rates [13][19]. In these studies the brush seal heat impact on the rotor disc has been calculated via infrared thermography of the rotor disc, and the adaption of finite elements analysis. Analytic correlations for plain rotating discs have been used as heat transfer boundary conditions [20][21]. None of the works reviewed provide correlations for the heat impact of brush seals for varying (non-eccentric) overlap conditions, as occurs through the thermal or rotational growth of a rotor. To account for an approach “as close as possible to real conditions”, it was decided to measure the effects of brush seal heat impact on disc temperature directly inside the rotor disc. This method requires thermocouples on the rotor surface and a telemetry system. The brush seal heat impact is afterwards calculated with an inverse approach by means of a finite elements simulation. In contrast to the available literature, the designed test rig should feature the possibility to accurately determine the boundary conditions for the finite elements analysis, e.g. with the help of insulating material inside the rotor.

As the test rig design strongly depends on the chosen measurement approach, an initial study has been carried out at the beginning of the project. The aim was to answer the question of whether the temperature measurements can be done at steady state conditions, or if a transient approach has to be applied. The results of the finite elements simulation of potential rotor designs showed, that the steady-state condition of a rubbing brush seal on a rotor with high rotational speed could not be achieved, even with a huge local cooling effort. Consequently, the test rig was designed for transient operation, meaning the main task was to record the transient heating of the rotor disc caused by the brush seal.

TEST RIG REQUIREMENTS

The brush seal frictional behavior and thus the heat impact into the rotor, the air, and the casing structure depend on a variety of influencing parameters.

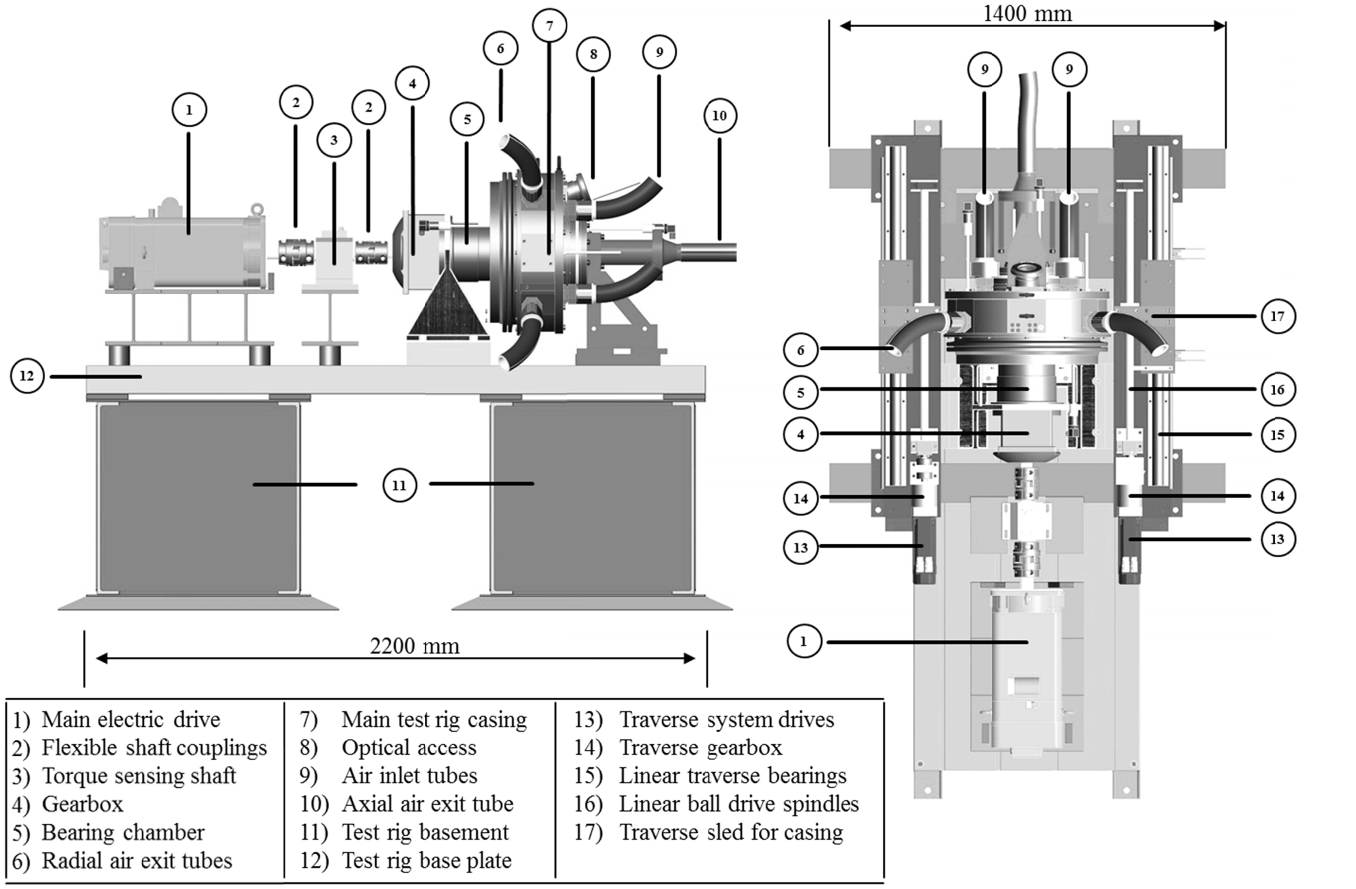

Fig. 4: Test rig design – global overview

These are mainly the rotational speed of the rotor, the degree of rotor-seal overlap, and the pressure drop induced air flow across the seal, which acts as a coolant for the seal and its environment. It was decided early on in the project to build a test rig which is able to simulate all major influences of a real engine. The specified test rig requirements were as follows:

- Differential pressure Δp→ variation from 1-10 bar
- Rotor speed u→ variation from 0 – 190 m/s
- Rotor – seal overlap Δs→ variation from 0 – 0.5 mm

The variation of rotor-seal overlap was decided to be accomplished via traversing the brush seal over a conically shaped rotor disc. Beyond that, the test rig should also allow for measurements of the important flow and brush seal dimensions, meaning all relevant air pressures, temperatures, and mass flows. Moreover, the necessary rotor drive torque and centricity of the rotor to the brush seal should be quantified. Most important, and in contrast to all presently available literature, it was decided to measure the heat impact on the rotor disc not via infrared thermography, but with a set of thermocouples directly installed beneath and as close to the brush seal rubbing surface as possible. In turn, this requires the installation of a multi-channel telemetry system, which transfers the temperature readings from the rotating system to the data acquisition unit. The telemetry electronics have to be installed in an environment with demanding conditions (high rotational speed, air pressure and mass flows), thus the telemetry mechanics need to be carefully designed in respect to their structural strength and pressure tightness. For simplicity, the test rig shall not be operated with hot air, which eases the choice of materials and measurement hardware.

TEST RIG DESIGN - OVERVIEW

The final test rig was assembled with some available parts donated by MTU Aero Engines (gearbox and bearing chamber) and the majority of new parts being manufactured at ITS or from suppliers. The design accounts for all specified test rig requirements and is suitable for a wide range of future brush seal research. The individual units of the test rig are mounted on a solid, sand-filled foundation weighing more than 4 tons. The arrangement can be seen in Fig. 4. An electric motor with 34 kW and 140 Nm drives the test rotor via a torque sensor shaft and a gearbox with a speed ratio of 1:7.2. The electric drive is rpm-controlled with a quick response control loop, and

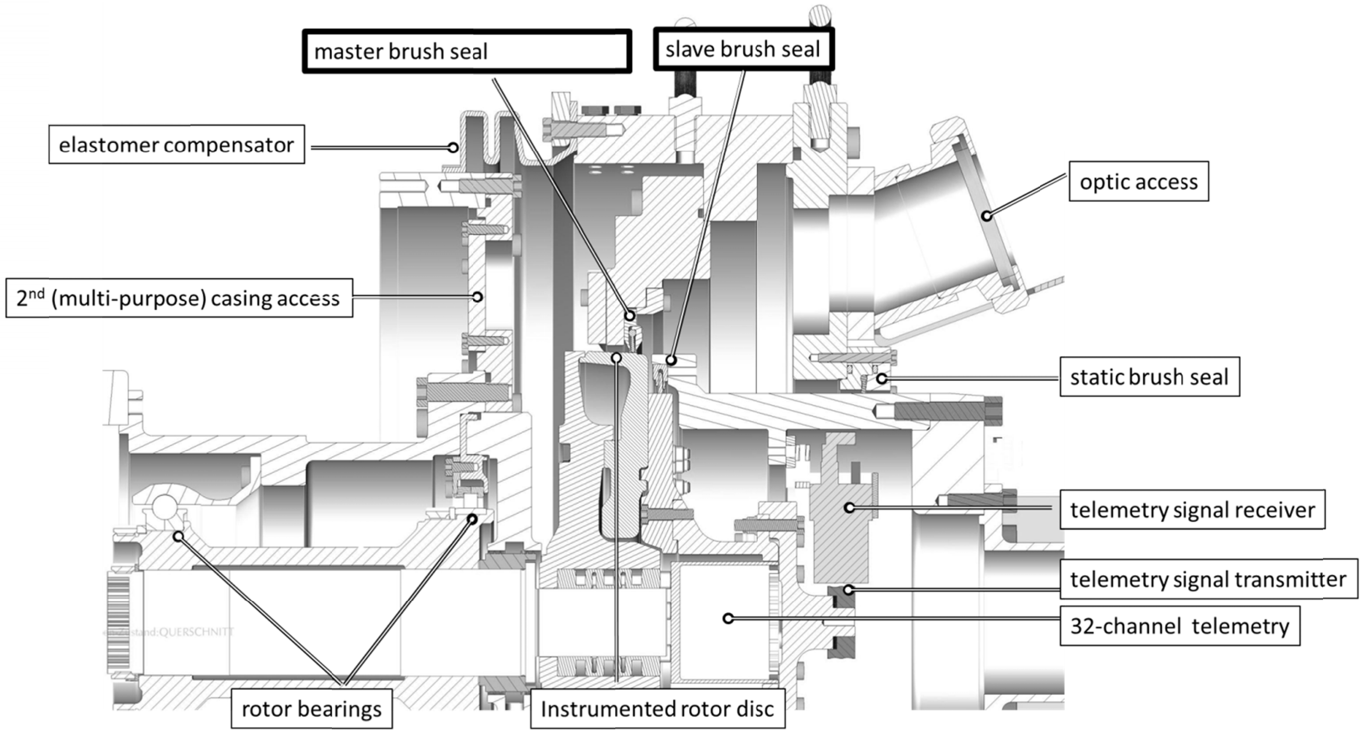

Fig. 5: Test rig casing - cut through optical access

maintains the rotational speed even when the necessary torque changes rapidly due to instant brush seal rubbing. The rotor is fully enclosed by a multi-part casing, which is not only necessary to establish the desired air pressure, but also serves as containment in case of rotor failure. The linear traverse system consists of two software-coupled, servomotor-driven linear traverse units, one on each rig side, and is capable of shifting a part of the casing axially over the rotor disc (the traverse system is only displayed on the right side in Fig. 4). As the brush seal is mounted in this traversed casing part, and the rotor is of conical shape, this relative motion varies the radial gap between the brush seal bristles and rotor disc.

TEST RIG DESIGN – CASING AND ROTOR

The arrangement of the casing parts and the rotor is displayed in Fig. 5. The casing consists of three main parts, which are the bearing chamber casing, the traversed casing, and the secondary casing. The stationary bearing chamber mainly contains the rotor shaft and the bearings. The traversed casing contains the tested brush seal (from now on referred to as "master brush seal"), and incorporates various measurement hardware. The secondary casing serves as a stiff support for the second brush seal (from now on referred to as "slave brush seal"). The slave brush seal is needed so as to have a second seal on the rotor surface of relatively high radius and thus to reduce the thrust on the ball bearings. A key issue in the casing design was to mechanically uncouple the master and the slave brush seal in a way that only the master brush seal is traversed on the rotor. Consequently only this brush seal creates frictional heat impact. The traversed parts of the casing have to be sealed against the static parts. A hermetically sealed elastomer compensator on the upper left casing and a static brush seal at the lower right casing are installed for that purpose. Moreover, this casing design allows a large optical access to the brush seal and a second multi-purpose access at the downstream side (see Fig. 5).

The pressurized air is fed into the rig casing through a set of four air inlet tubes at the right side of the traversed casing. The air then passes through the master brush seal and exits the casing radially, again through a set of four tubes. Air which passes though the slave brush seal exits through the secondary casing and through one large diameter tube (Fig. 6).

The overhung rotor with an outer diameter of 300 mm is supported by a ball bearing and a roller bearing, and is composed of a conically shaped Inconel 718 disc, which is enclosed by additional parts made from X11CrNiMo12. A telemetry system is attached to the rotor, which collects and processes temperature data from 12 thermocouple positions. The data is transferred into the static system via a pair of contactless transmitter / receiver coils. The rotor was designed by means of finite elements analysis. The main focus was put on high structural strength, only aircraft certified material with appropriate heat treatment was used. The maximum rotational speed with the actual rotor is 12.000 rpm, leading to about 190m/s at 300 mm diameter. A second rotor with a possible rotational speed of 300 m/s has already been designed, and

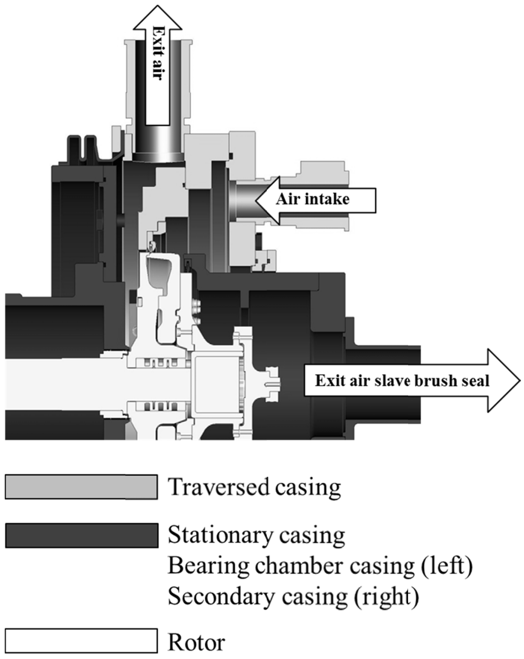

Fig. 6: Cross section of test rig

partly manufactured. This second rotor will be installed in the near future, in order to extend the possible operating conditions.

EXPERIMENTAL INFRASTRUCTURE

Air supply

The test rig is connected to the ITS compressor network, which is fed by three screw-type compressors (Fig. 7). When operated together, the system delivers a mass flow of up to 700 g/s with up to 10 bar absolute pressure. Air temperature is kept at a level of 40°C after compression. After feeding a pressure vessel, the air is channeled in either a DN50 or a DN80 pipe duct, where the mass flow to the test rig is metered via differential pressure orifices. Exit air mass flow is metered via hot film mass flow metering devices in both ducts. The pressure drop over the brush seal is adjusted with the help of the automatically controlled bypass system. After passing the test rig the air is collected in the exit air duct, and leaves the network through an outlet system.

Oil system

The rotor bearings and the gearbox are lubricated with oil jets. The oil serves as a heat sink rather than being needed for lubrication purposes, which is due to the high rotor thrust acting on the fixed bearing and the high amount of frictional torque inside the gearbox. Consequently a water-oil heat exchanger was installed which maintains constant oil temperature.

MEASUREMENT AND CONTROL INFRASTRUCTURE

The test rig is equipped with a large number of sensors in order to detect and record the important parameters regarding

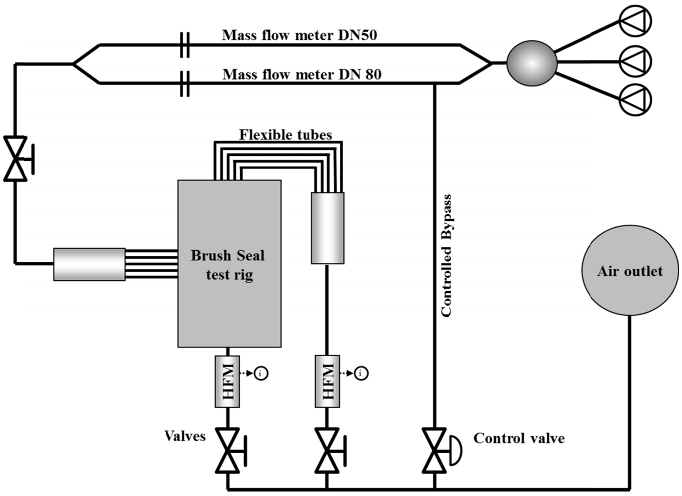

Fig. 7: Air supply network of brush seal test rig

brush seal behavior and test rig control (see Table 1). The following parameters are measured:

- Temperature of the rotor structure at 12 positions, VHF-transmission with telemetry (see Fig. 8).
- Air temperature upstream of brush seals and downstream of each brush seal, measured inside the test rig casing.
- Bearing temperature at both bearings at outer ring.
- Air pressure upstream of brush seals and downstream of each brush seal, measured inside the test rig casing.
- Air pressure of sealing air and inside bearing chamber.
- All relevant mass flows (upstream and downstream of brush seal, sealing air mass flow).
- Torque of main electric drive (before transmission).
- Rotational speed of rotor disc.
- Centricity and distance of brush seal from rotor surface via set of three capacitive distance sensors.

The mass flow and pressure sensors were calibrated using professional calibration devices.

The test rig control and data acquisition system is – for safety reasons - basically distributed on two PCs. All measurement data is multiplexed and processed by a National Instruments SCXI multi-slot system, subsequently the A/D conversion is carried out by a PCI card which is located in the PC. This computer records all data, monitors the test rig condition with a graphical user interface (LabView) and gives

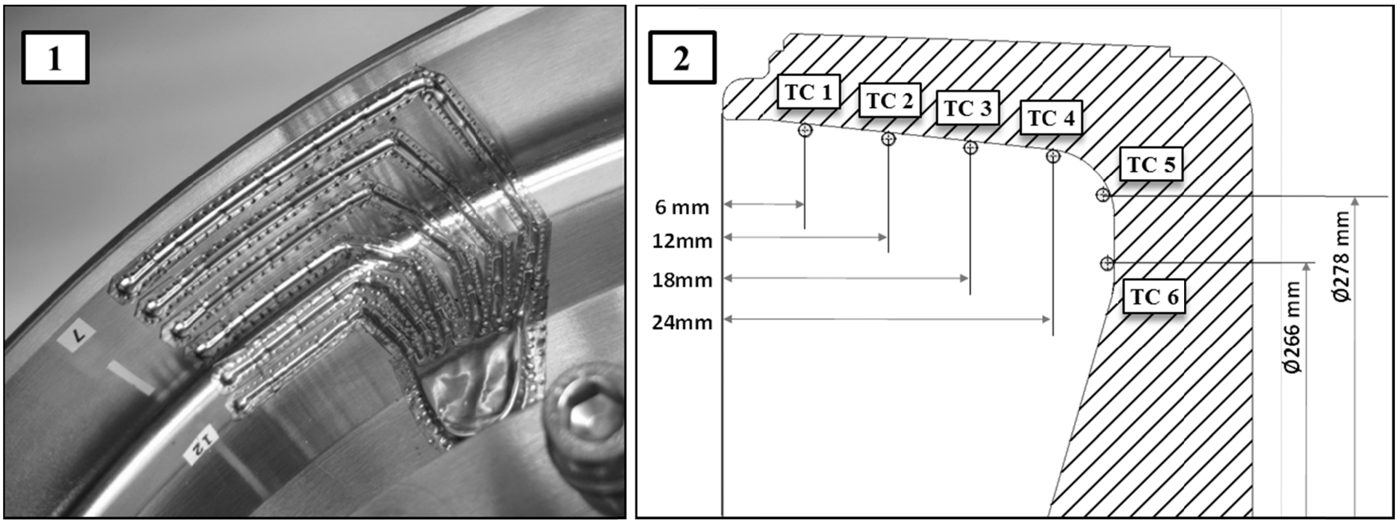

Fig. 8: Rotor instrumentation
1) Shielded thermocouple alignment, 2) Distribution of thermocouples

Table 1: Technical data of drive system and sensors

Drive Systems	Torque	Power	RPM	Misc.
Main electric drive	140 Nm	34 kW	3000 RPM	
Traverse drives (2x)	5.88 Nm	2.5 kW	4000 RPM	Traverse speed up to 120 mm/s with forces up to 40 kN

Sensors	Signal	Range	Accuracy
DATATEL telemetry system, 32 channel, 1Hz per channel	-6.5 mV – 54.8 mV	-270°C – 1372°C	+/- 2 K
Thermocouples Type K	-6.5 mV – 54.8 mV	-270°C – 1372°C	+/- 0.5 K
Pressure sensor downstream + bearing chamber (Wika S-10)	4 mA – 20 mA	0 – 1.6 bar (abs)	+/- 0.008 bar
Pressure sensor upstream (WIKA S-10)	4 mA – 20 mA	0 – 10 bar (abs)	+/- 0.05 bar
Differential pressure at orifice DN 80 / DN 50 (Druck PMP)	0 V – 2 V	0 – 70 mbar	+/- 0.35 mbar
Absolute pressure at orifice DN 80 / DN 50 (Druck PMP)	0 V – 10 V	0 – 8 bar (abs)	+/- 0.04 bar
Bosch mass flow meter HFM5 (master seal exit air)	0 V – 5 V	0 – 333 g/s	+/- 10 g/s
Bosch mass flow meter HFM5 (slave seal exit + sealing air)	0 V – 5 V	0 – 133 g/s	+/- 4 g/s
Capacitive distance sensors (Capa NCDT 6100/CS1HP)	0 V – 10 V	0 – 1 mm	+/- 0.003 mm
Torque sensor shaft (Lorenz DR-2212)	+/- 5 V	0 – 500 Nm	+/- 0.5 Nm
Shaft rotational speed before gearbox (Lorenz DR-2212)	TTL	0 – 7000 RPM	+/- 5 RPM
Position sensor for traverse system (WPS-1000-MK46)	% of ref. voltage	1000 mm	+/- 0,3 mm

warnings to the user if inappropriate operating conditions occur. The second computer serves solely as a host system to control the traverse system.

TYPICAL OPERATION

Each specific point of operation includes a specific condition for pressure drop, rotor rotational speed and rotor-seal overlap. The test procedure for one such operation point consists of the following steps. At first, the test rig is taken into operation with all relevant measurement, control and drive devices. Subsequently, the brush seal is traversed on the lowest position on the rotor cone, corresponding to an effective gap of 0.1mm. Afterwards the bypass of the air feed duct is gradually closed until the air pressure upstream of the brush seal is raised at least on a level which creates a rotor thrust of 5 kN. This is a requirement for safe use of the bearings at significant rotational speed. Now the rotor can be accelerated to the desired rotational speed for this operation point, while the air pressure is adjusted to its designated level. The test rig is then operated for the time span

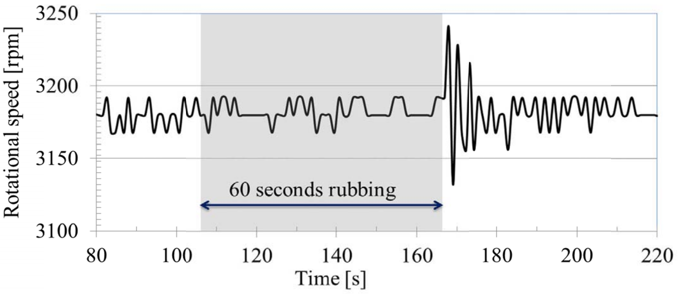

Fig. 9: Rotor rotational speed

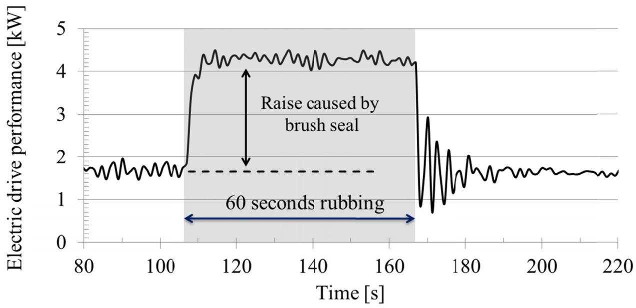

Fig. 10: Performance of electric drive

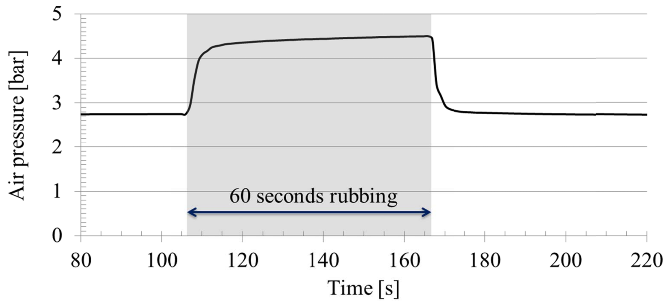

Fig. 11: Air pressure upstream of brush seal

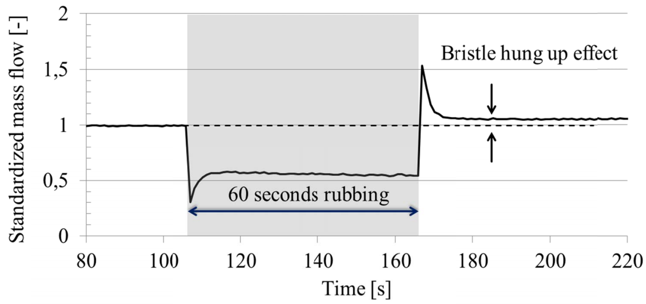

Fig. 12: Leakage mass flow across brush seal

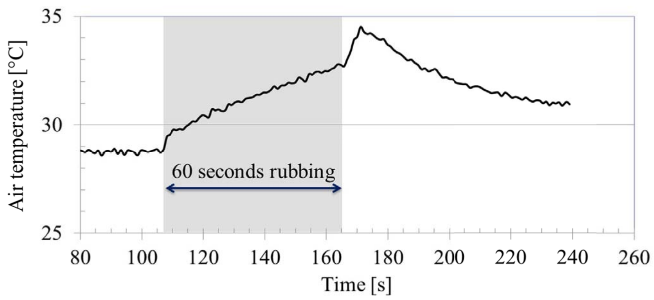

Fig. 13: Air temperature downstream of brush seal

Δt_1 until all measurements have reached steady-state. This is necessary to clearly separate between all unsteady effects which arise through the intentional brush seal rubbing and unsteady effects which occur until the test rig reaches its desired steady operational point. Subsequently the brush seal is traversed on its target position on the rotor cone, corresponding to a specific overlap for each position. The target position also depends on the operation conditions. Analyses in finite elements showed that the rotor expands radially with centrifugal forces (up to 0.3 mm) and is exposed to radial thermal growth (up to 0.1 mm).The centrifugal growth is taken into consideration through monitoring the current rotor diameter with a set of three capacitive distance sensors. The target position for the brush seal rubbing is consequently chosen depending on the actual growth, so that the desired overlap is identical for different rotational speeds. The thermal growth is not taken into consideration until now, as it can be neglected for low brush seal heat impact. Yet it needs to be considered for strong brush seal rubbing conditions. For the future it is planned to account for thermal growth by means of prior analyses by finite elements.

The traverse system was designed to shift the brush seal on every possible position in less than 0.2 s, while it has to counteract the casing pressure force of up to 17 kN. The quick traverse leads to a minimization of undefined heat generation while the brush seal moves over the rotor cone to its target position. With an increased overlap, the sealing behavior is improved which leads to a reduced air mass flow across the seal. Consequently the upstream air pressure needs to be kept constant by controlling the bypass in the air feed duct.

During the controlled rubbing period of the brush seal on the rotor surface, the temperature readings of the 12 rotor thermocouples are recorded with a frequency of 1 Hz. All further measurements can be recorded with virtually unlimited frequency (several kHz if necessary) considering the temporal resolution of the sensor electronics. The rubbing process is stopped after a time span Δt_2 by traversing the casing back to its initial position. Δt_2 is defined through the designated maximum material temperature of 650°C at the rubbing location. The structural temperature at this position cannot be measured directly, so Δt_2 must be calculated through finite elements analyses prior to the experiments, at least for the operation points with high rotational speed and high overlap, where Δt_2 can be as low as 6 seconds. For low rotational speed and/or small overlap, the heat impact is expected to be low, resulting in a slow and uncritical rotor temperature increase.

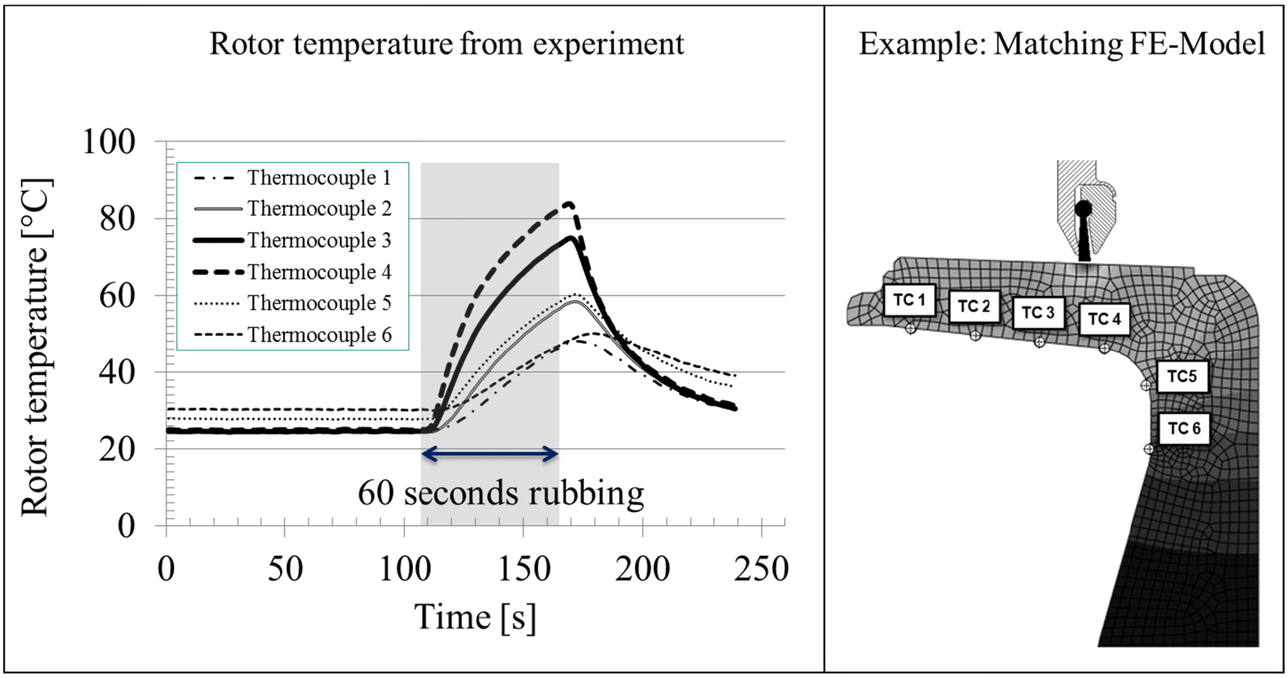

Fig. 14: Transient rotor temperatures and corresponding example of finite elements model

Although it would be possible to choose a long rubbing time span for such conditions, it is no use expanding Δt_2 to more than 60 seconds, as this is more than enough to get sufficient transient temperature information. After the casing is traversed back to its initial position, the test rig is further operated with the designated operation point, until steady-state is reached again

During this last time period Δt_3 of the experiment, it is possible to gather information about the relaxation behavior (and a possible hang up effect) of the bristles. All test rig operation is recorded with a video camera through the optical access. These recordings can give information about blow-down behavior of the seal. As an option, in future the video camera could be replaced by an infrared camera, giving local temperature data of the brush seal casing and bristles.

RESULTS

The complete test rig was used for a series of validation runs and the preliminary results proving the functionality of all major components will be reported in the following section. The results were achieved with an experimental rubbing test with a fully operational test rig, meaning with relevant rotational speed, pressure ratio and overlap. The test procedure was as described in chapter “TYPICAL OPERATION” with a rotor speed of 50 m/s (corresponding to 3180 rpm), a differential pressure across the seal of 1.7 bar and an overlap of 0.1mm.

As can be seen in Fig. 9, the rotational speed of the rotor was basically constant during the rubbing period but shows a small oscillation after the brush seal is traversed back to its initial position. The necessary mechanical drive power of the main drive is displayed in Fig. 10, revealing a rise of approximately 2.5 kW, which is caused through the brush seal interference. This additional power was dissipated in the heating up of the rotor, casing, air, and the mechanical abrasion of the bristles.

Air pressure upstream of the brush seal is shown in Fig. 11. For the future experiments, the bypass control of the test rig will be optimized to keep the upstream air pressure as constant as possible, as it is an important parameter for brush seal thermal behavior. Unfortunately, the bypass was not working properly during the test run shown here. Consequently the pressure increased during the brush seal rubbing through the improved sealing behavior. After the rubbing was finished, the pressure level recovered.

Due to the increasing pressure during the rubbing period, the mass flow through the seal (Fig. 12) needs to be interpreted carefully. First, it is displayed as a standardized value, which means it was scaled to its initial value prior to the rubbing process. Immediately after the brush seal was traversed on the interference location on the conical rotor, the mass flow decreased. This effect is expected, since a rotor-seal overlap means a reduced gap between the backing plate and rotor. The gap size has a great effect on the brush seal leakage, as it represents the relevant flow cross-section which is blocked by the bristles. During the rubbing, the changing upstream air pressure affected the leakage. After the rubbing was finished, the leakage recovers with a slightly higher value. This could be interpreted as a hang up effect of the bristles, which was already widely discussed in literature, e.g. [16][22].

Fig. 13 shows the rising air temperature downstream of the brush seal, which shows a maximum soon after the brush seal rubbing is finished. Finally, Fig. 14 gives the most interesting part of the measurements, which are the transient temperature readings from the rotor. The rotor is equipped with 2 x 6 thermocouples, the two instrumented regions are displaced 180° circumferentially for reasons of thermocouple redundancy and rotor balancing. As the readings from both instrumented regions are identical, only 6 thermocouple readings from one of the two instrumented regions are shown in Fig. 14.

It can be seen from the temperature distribution in Fig. 14 that the initial thermal condition of the rotor does not seem to be completely isothermal, but stationary. This is most probably due to windage heating around the slave brush seal. The closest thermocouples to the slave seal are thermocouple TC 5 and TC 6, which would explain why these two readings start at a slightly higher temperature level than the other readings. After the rubbing process started, the temperature readings increased with differing delays, depending on the distance from the heat impact position. Thermocouples 3 + 4 are directly underneath the rubbing position, and faced the fastest and strongest temperature increase, followed by thermocouples 2 + 5, while the readings from thermocouples 1 + 6 show a delayed and smaller temperature increase. After the brush seal was traversed back to its initial position, the temperature decreased, depending on the thermocouple position with no or slight delay time.

CONCLUSIONS

A newly designed and built versatile test rig for brush seal behavior, particularly for rubbing conditions, was presented in this paper. The main focus of the new rig at the ITS was on the frictional heat generation of brush seals during rotor-seal contact, which is measured in-situ through a thermocouple instrumented rotor disc. The rig allows the combination of engine-like operation conditions with the possibility to vary the radial gap between the brush seal and the rotor. Preliminary experimental results proved the functionality of the complex design, which will be used in future to test different brush seals in a variety of operating conditions. The determination of the brush seal heat impact on the rotor will be carried out with an inverse approach by comparing experimental temperature readings with a finite elements model. The boundary conditions for this model have to be carefully assigned; a sensitivity analysis of the various boundary conditions will follow. The test rig eases this task as the rotor design offers the possibility to insert insulation material inside the rotor disc. The data obtained from the future brush seal research in Karlsruhe will be used to setup correlations and mathematical models to thoroughly understand the tribology and heat generation of brush seals

ACKNOWLEDGMENTS

This scientific publication is the result of a research project which has been initiated by the FVV ("Forschungsvereinigung Verbrennungskraftmaschinen") and carried out at the Institut für Thermische Strömungsmaschinen, Karlsruhe Institute of Technology. The work has been supported financially by the FVV and the participating companies. This support is gratefully acknowledged, moreover the authors thank the representatives from various participating companies who contributed with technical assistance during project meetings. Special thanks go to Mr. Hans Göttler (MTU Aero Engines), who served as project chair and coordinated important technical communication between all partners.

REFERENCES

[1] Steinetz, B.M. and Hendricks, R.C., 1997. "Engine seals". In: E.V. Zaretsky (ed.) Tribology for Aerospace Applications, Society of Tribologists and Lubrication Engineers, pp. 595-682.

[2] Arora, G.K. and Proctor, M.P., 1997. "JTAGG II Brush seal test results". NASA TM 107448, AIAA-97-2632, ARL-TR-1397.

[3] Proctor, M.P. and Delgado, I.R., 2004. "Leakage and power loss test results for competing turbine engine seals". ASME-Paper No. GT2004-53935.

[4] Conner, K.J. and Childs, D.W., 1993. "Rotordynamic coefficient test results for a four-stage brush seal". Journal of Propulsion and Power, 9(3), pp. 462-465.

[5] Chupp, R.E., Ghasripoor, F., Turnquist, N.A., Demiroglu, M. and Aksit, M.F., 2002. "Advanced seals for industrial turbine applications: Dynamic seal development". Journal of Propulsion and Power, 18(6), pp. 160-166.

[6] Ferguson, J.G., 1988. "Brushes as high performance gas turbine seals". Int. Gas Turbine and Aeroengine Congress, ASME-Paper No. 88-GT-182.

[7] Neef, M., Sulda, E., Sürken, N. and Walkenhorst, J., 2006. "Design features and performance details of brush seals for turbine applications". ASME-Paper No. GT2006-90404.

[8] Gail, A. and Beichl, S., 2000. "MTU Brush Seal – Main features of an alternative design". AIAA 2000-3375

[9] Information brochure of MTU Aero Engines GmbH, Munich, Germany, 2006. "Brush seals – Precision and know-how to meet exacting requirements".

[10] Rolls-Royce plc., 2005. "The Jet Engine". ISBN: 0 902121 235.

[11] Franceschini, G., Jones, T.V. and Gillespie, D.R., 2008. "Improved understanding of blow-down in filament seals". ASME-Paper No. GT2008-51197.

[12] Pröstler, S., 2004. "Modellierung und numerische Berechnung von Wellendichtungen in Bürstenbauart". PhD Thesis, University of Bochum, Germany.

[13] Owen, A.K., Jones, T.V., Guo, S.M., 2003. "An experimental and theoretical study of brush seal and shaft thermal interaction". ASME-Paper No.GT2003-38276.

[14] Hendricks, R., Schlumberger, S., Braun, M.J., Choy, F. and Mussen, R.L., 1991. "A bulk flow model of a brush seal system". Gas Turbine and Aero Engine Congress and Exposition, ASME-Paper No. 91-GT-325.

[15] Dogu, Y. and Aksit, M.F., 2005. "Brush seal temperature distribution analysis". ASME-Paper No. GT2005-69120.

[16] Demiroglu, M., Gursoy, M. and Tichy, J.A., 2007. "An investigation of tip force characteristics of brush seals". ASME-Paper No.GT-2007-28042.

[17] Long, C.A. and Marras, Y., 1995. "Contact force measurements under a brush seal". International Gas Turbine and Aeroengine Congress and Exhibition, Houston, Texas, ASME-Paper No. 95-GT-211.

[18] Franceschini, G., Morgan, J.J., Jones, T.V., Gillespie, D.R., 2006. "A slow-speed rotating test facility for characterising the stiffness of brush seals". ASME-Paper No. GT2006-91335.

[19] Demiroglu, M. and Tichy, J.A., 2007. "An investigation of heat generation characteristics of brush seals". ASME-Paper No. GT2007-28043.

[20] Dorfman, L.A., 1963. "Hydrodynamic Resistance and the Heat Loss of Rotating Solids". Olivier and Boyd, Edinburgh.

[21] Northrop, A., Owen, J.M, 1988. "Heat Transfer Measurements in Rotating-disk Systems, Part 1: The Free Disk". Int. J. Heat and Fluid Flow, 9(1), pp.19-26.

[22] Basu, P., Datta, A., Johnson, R., Loewenthal, R. and Short, J., 1996. "Hysteresis and Bristle Stiffening Effects of Conventional Brush Seals". AIAA No. 93-1996.

